Proceedings of the 21st ICSMGE, Vienna, Austria, 14 – 19 June 2026. Pistrol, Adam & Schweiger (eds.)
Published by: ÖGG, Austrian Society for Geomechanics, Salzburg, Austria, ISBN 978-3-9503898-4-5
https://doi.org/10.53243/ICSMGE2026-290

Measured and predicted dynamic response of an embedded footing

Dennis R. Hiltunen
Department of Civil and Coastal Engineering, University of Florida, U.S.A., dhilt@ce.ufl.edu

ABSTRACT: A shallow foundation, 3 m x 3 m in plan and embedded 0.9 m, was dynamically loaded at the National Geotechnical Experiment Site (NGES) on the campus of Texas A&M University (TAMU) and the measured results were compared with results computed via four widely publicized methodologies. The measured responses of the footing indicated that a rigid body motion model for movement of the footing was appropriate. This rigid body model based upon both single- and two-degree-of-freedom (SDOF), mass-spring-dashpot concepts, employing computed dynamic impedance functions, and using free-field shear wave velocity values measured at the site with surface wave tests, provided predictions of the dynamic response. The cone models produced the best predictions of the measured field response and all four methodologies produced good predictions of the vertical and horizontal motions of the foundation. The rocking motions were well predicted using cone and half-space models, while the PILAY predictions of rocking were quite different from the measurements. The Gazetas model results suggested that full embedment and full contact of the foundation and soil produced the best representation of the field behavior. It was possible to find one representative half-space modulus for the models to match the field measurements for all modes of vibration, but it was not obvious how one would determine this modulus value a priori in a design situation and without the benefit of field response measurements.

KEYWORDS: Footing, embedded, dynamic, impedances, predicted.

1 INTRODUCTION

Recent decades of research have produced significant advancements in both laboratory and in situ characterization of geotechnical sites, and in methodologies for the prediction of dynamic foundation behavior. Many numerical methods have been compared to the few exact solutions available and to each other, but few have been compared with carefully performed, full-scale tests of dynamically loaded embedded footings on well characterized soils (Tileylioglu, Stewart, and Nigbor 2011). Yet, these methods are the starting points for virtually all calculations of dynamic foundation response, from sensitive instrument bases to earthquake shaking analyses.

A square and embedded shallow foundation has been dynamically loaded at the National Geotechnical Experiment Site (NGES) on the campus of Texas A&M University (TAMU). The dynamic load and vibration responses of the foundation were measured via appropriate electronic instrumentation. Utilizing appropriate equations of motion and system parameters, the measured load, and appropriate site characterization data and material properties, dynamic foundation responses were predicted for the vertical, horizontal sliding, and rocking modes of vibration via four widely publicized methodologies. Also, a parametric study of the effect of half-space modulus and the effect of embedment were conducted via the Gazetas (1991) model to compare with the field measured data. The paper presents a comparison of the model predictions with measurement results from the physical experiments.

2 FOUNDATION, SHAKER AND SITE DESCRIPTIONS

A shallow foundation, 3 m x 3 m in plan and embedded 0.9 m, was loaded at the National Geotechnical Experiment Site (NGES) on the campus of Texas A&M University (TAMU) via two dynamic shakers: the NSF NEHRI "T-Rex" mobile shaker operated by the University of Texas and an ANCO Model MK-12 rotating mass vibrator with a maximum applied load of 44.5 kN (10,000 lb), and a frequency range from 0 to 100 Hz. The TAMU NGES site has been extensively characterized via both in situ and laboratory soil testing techniques (Briaud and Gibbons 1994), including shear wave velocity via both borehole and surface wave methods (Tran and Hiltunen 2011). The site consists of an upper layer of approximately 10 m (32.8 ft) of medium dense, silty, fine sand followed by hard clay. The water table is approximately 5 m (16.4 ft) below the ground surface.

3 FOOTING RESPONSE MEASUREMENTS

3.1 *Vertical*

Figures 1-4 present an experiment for the vertical loading of the 3 m x 3 m footing using the T-Rex shaker configured to load in the vertical direction. The magnitude of the load was determined by an Interface Model 1240 load cell exhibited in Figure 1. The photograph also displays three velocity transducers deployed at each of the four corners of the footing surface for measurement of the footing response to load.

Figure 1. Vertical loading experiment photograph.

Figure 2 displays the amplitude of vertical load as frequency increases. The resulting vertical displacement response of the foundation is displayed in Figures 3 and 4. The complex number (real and imaginary) format implicitly contains both the amplitude of the sinusoidal displacement response, as well as the phase lag of the displacement from the applied sinusoidal loading. In operation, the loading was conducted in a steady-state mode wherein several cycles of load were applied at a constant frequency, beginning at the lowest frequency. The dynamic response of the foundation was measured simultaneously via the velocity transducers and recorded via a dynamic signal analyzer capable of characterizing the signals in complex number format. The displacement response was determined by integration of the velocity transducer measurements, and the loading was repeated at small increments of frequency through the frequency range noted in Figures 2-4. Finally, it is noted that the displacement responses are displayed for each of the four corners of the foundation. The four responses are indeed very similar, which in part indicates that the foundation is moving vertically in a rigid-body-like fashion.

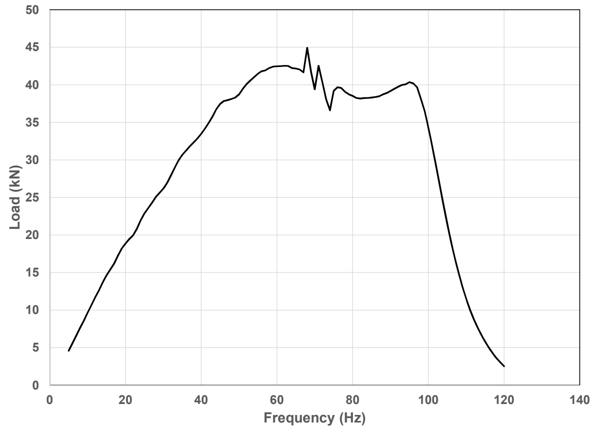

Figure 2. Vertical load.

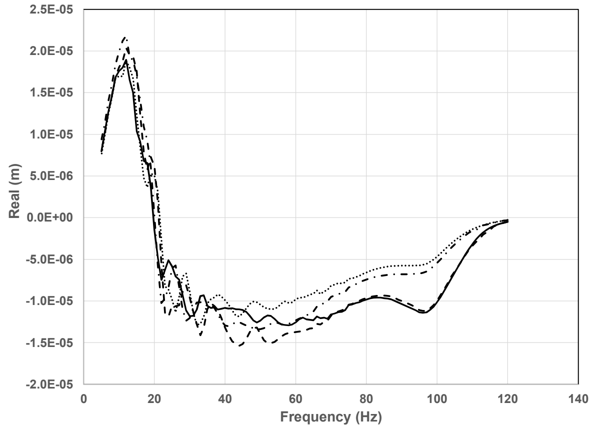

Figure 3. Vertical displacement real component.

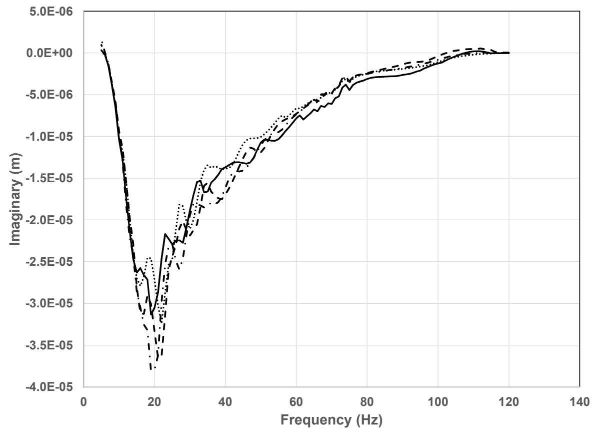

Figure 4. Vertical displacement imaginary component.

3.2 *Horizontal*

Figures 5-10 present an experiment for the horizontal loading of the 3 m x 3 m footing using an ANCO Model MK-12 rotating mass shaker configured to load in the horizontal direction. The horizontal loading was performed with the shaker attached directly to the foundation as illustrated in Figure 5. The magnitude of the load was determined by the speed and eccentricity settings of the rotating masses. The photograph also displays three Geospace GS-1 velocity transducers deployed at each of the four corners of the footing surface for measurement of the footing response to load.

Figure 5. Horizontal loading experiment photograph.

Figure 6 displays continuously increasing amplitude of horizontal load as frequency increases, which is characteristic behavior for a rotating-mass-type shaker. The resulting horizontal and vertical displacement responses of the foundation top surface are displayed in Figures 7-10. The complex number (real and imaginary) format implicitly contains both the amplitude of the sinusoidal displacement response, as well as the phase lag of the displacement from the applied sinusoidal loading. In operation, the loading was conducted in a steady-state mode wherein several cycles of load were applied at a constant frequency, beginning at the lowest frequency. The dynamic response of the foundation was measured simultaneously via the velocity transducers and recorded via a dynamic signal analyzer capable of characterizing the signals in complex number format. The displacement response was determined by integration of the velocity transducer measurements, and the loading was repeated at small increments of frequency through the frequency range noted in Figures 6-10. The responses at each of the foundation corners are presented individually in the figures. It should be noted that the four horizontal displacements shown in Figures 7 and 8 are very similar, which in part indicates that the foundation is moving horizontally in a rigid-body-like fashion.

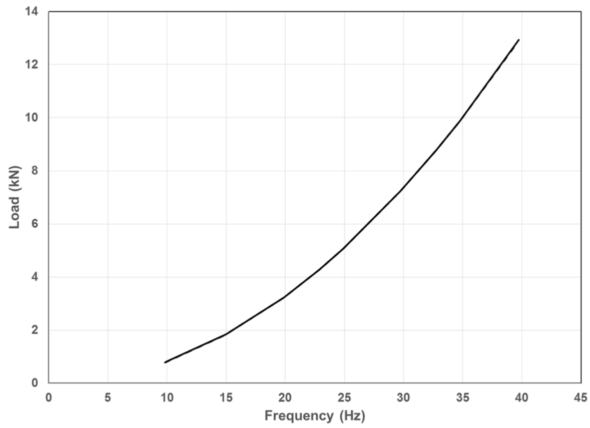

Figure 6. Horizontal load.

The vertical displacements shown in Figures 9 and 10 are due to the rocking motion of the foundation. Here, it is observed that there are two pairs of similar data for each shaker arrangement. The similar responses are for the two corners along a foundation edge that is parallel to the axis of rocking. Of course, there are two such edges, and they are each on opposite sides of the axis of rocking. These responses should be at similar amplitude, but 180 degrees out of phase if the rocking axis is contained in the same vertical plane as the center of the foundation. Indeed, the data possess this symmetry: the real and imaginary pairs are both of similar magnitude, but opposite in sign (i.e., 180 degrees out of phase). This behavior also suggests a rigid-body-like rocking motion, and with this as an assumption, the rotation of the foundation can be calculated from the geometry and the vertical displacement responses.

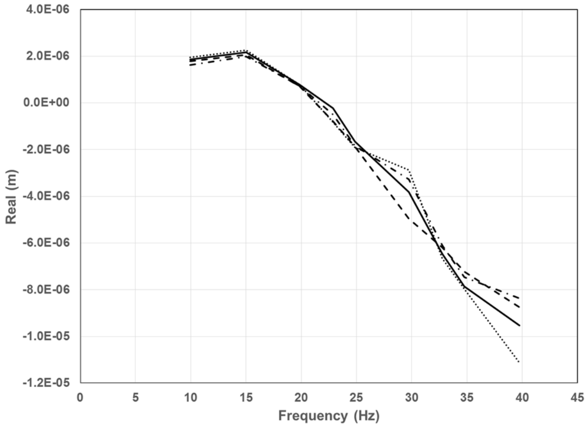

Figure 7. Horizontal displacement real component.

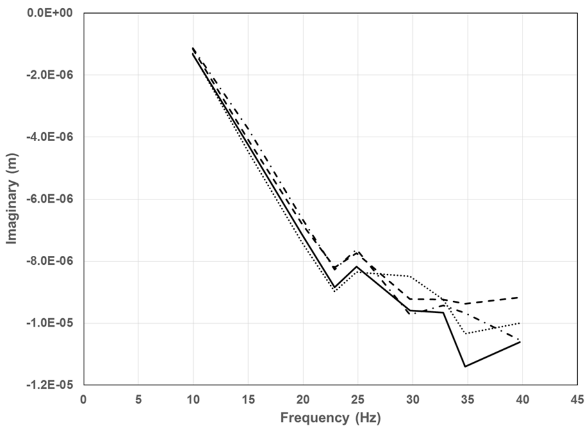

Figure 8. Horizontal displacement imaginary component.

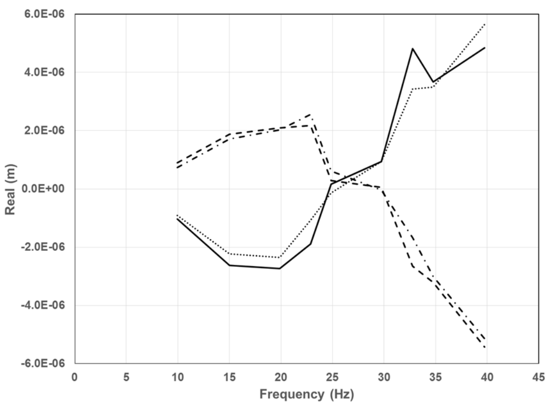

Figure 9. Vertical displacement real component.

4 PREDICTIONS OF FOUNDATION MOTIONS

Dynamic foundation motions were predicted via four widely publicized methodologies: the cone models of Wolf and Deeks (2004), the PILAY models of Novak and Aboul-Ella (1977, 1978), and the homogeneous half-space models for embedded footings of Apsel and Luco (1987) and Gazetas (1991). Figures 11-16 present measured versus predicted dynamic motion results for the two shaker experiments described in the previous section. The vertical displacements of the footing are displayed in the typical complex number format of magnitude and phase angle. The horizontal displacements presented are the movement of the center of gravity of the foundation system and are also displayed in the complex number format of magnitude and phase angle. Similarly, the rotations presented are the angular or rocking movement of the foundation about an axis passing through the center of gravity.

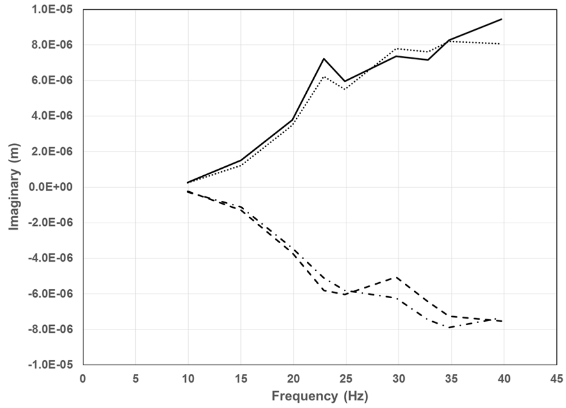

Figure 10. Vertical displacement imaginary component.

The measured vertical displacements shown in Figures 11 and 12 were computed as the arithmetic average of the four corner displacements measured under the loading of the T-Rex shaker (Figure 1). The predicted vertical displacements were computed using a a single-degree-of-freedom (SDOF), mass-spring-dashpot model of the soil/foundation system (Gazetas 1991, Wolf and Deeks 2004), which produces an equation for the vertical displacement as follows:

$$U_v = \frac{F_s}{S_v} \quad (1)$$

where: U_v is the vertical displacement of the model as a function of frequency, F_s is the force imparted on the soil by the foundation (in this case, the sum of applied loading from shaker and the inertia force of moving foundation), and S_v is the frequency-dependent dynamic impedance function for vertical motion of the soil/foundation system. The impedance function was determined via each of the models described below.

The measured horizontal displacement of the foundation center of gravity shown in Figures 13 and 14 were computed as the arithmetic average of the four corner top-surface displacements measured under the loading of the ANCO shaker (Figure 5) minus the horizontal movement of the foundation top surface created by the simultaneous rocking of the foundation.

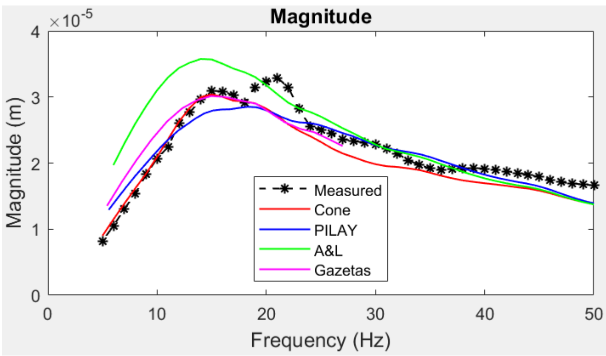

Figure 11. Vertical displacement magnitude.

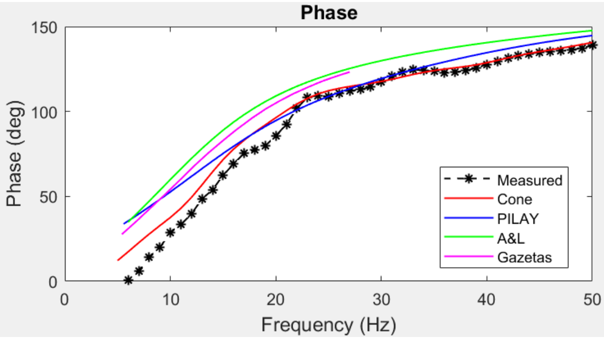

Figure 12. Vertical displacement phase angle.

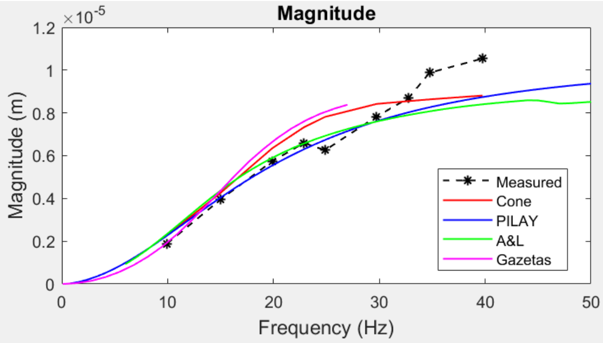

Figure 13. Horizontal displacement magnitude.

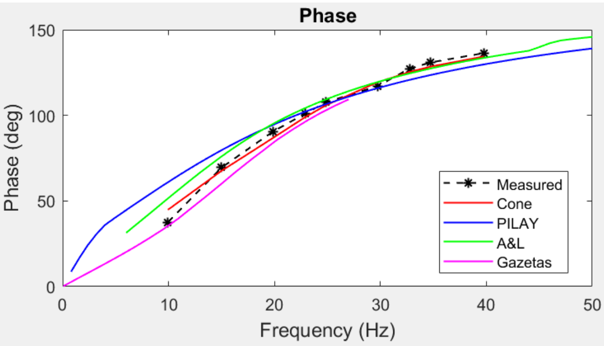

Figure 14. Horizontal displacement phase angle

The measured rotations of the foundation about the center of gravity shown in Figures 15 and 16 were computed from the vertical displacements under the horizontal loading of the ANCO shaker. First, the arithmetic averages of the two corner displacements along each foundation edge parallel to the axis of rocking were computed. Second, the rotation was computed as the inverse tangent of one-half the difference between the two arithmetic average vertical displacements divided by the distance between the two sets of geophones (approximately the width of the footing).

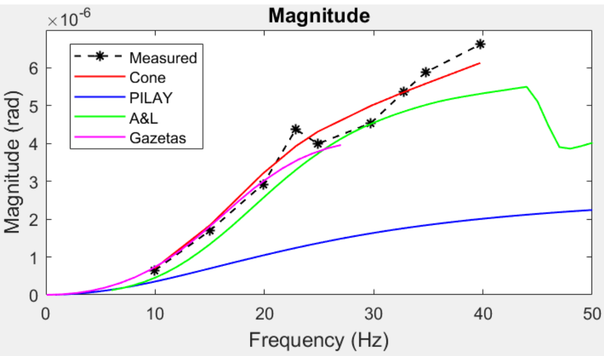

Figure 15. Rotation magnitude.

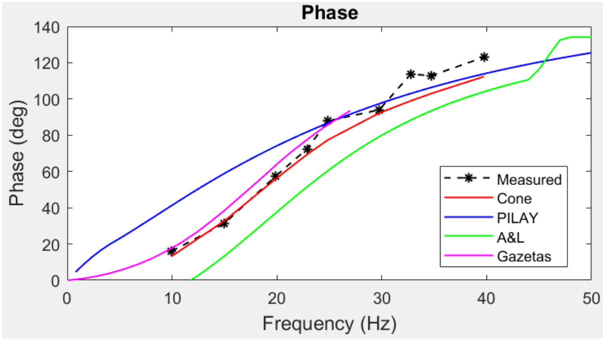

Figure 16. Rotation phase angle.

Since the horizontal loading of the ANCO shaker produced coupled horizontal sliding displacement and rocking rotation of the foundation, the predicted responses were computed using a rigid body, two-degree-of-freedom (2DOF), mass-spring-dashpot model of the soil/foundation system (Wolf and Deeks 2004), which produces the following matrix equation for the coupled motions:

$$\begin{bmatrix} u_{CG} \\ \theta_o \end{bmatrix} = \begin{bmatrix} \{-\omega^2 m + S_h\} & \{S_{hr} - eS_h\} \\ \{S_{rh} - eS_h\} & \{-\omega^2 I + S_r + e^2 S_h - e(S_{hr} + S_{rh})\} \end{bmatrix}^{-1} \begin{bmatrix} Q \\ M \end{bmatrix} \qquad (2)$$

where: u_{CG} is the horizontal displacement of the foundation center of gravity as a function of frequency, θ_o is the rotation of the foundation about the center of gravity as a function of frequency, Q is the horizontal force imparted on the foundation center of gravity (in this case, the applied loading from shaker), M is the moment imparted about the foundation center of gravity (in this case, the applied loading from shaker times vertical distance from shaker to center of gravity), m is the total mass of the foundation system, I is the mass moment of inertia of foundation about an axis passing through center of gravity, e is the vertical distance from base of foundation to the center of gravity, ω is the circular frequency, and S_h, S_r, S_{hr}, and S_{rh} are the frequency-dependent dynamic impedance functions for the horizontal (h), rocking (r), and coupled (hr and rh) motions of the soil/foundation system. The impedance functions were determined via each of the models described below.

4.1 *Cone Models*

The cone model solutions presented by Wolf and Deeks (2004) assume that foundation vibrations create one-dimensional, downward wave propagation in the supporting soil that is contained within a vertical cone of material whose top is truncated, and with a base area that increases with depth. For each degree of freedom, only one type of body wave exists: for the horizontal and torsional motions, S-waves propagating with the shear-wave velocity; and for the vertical and rocking motions, P-waves propagating with the dilatational-wave velocity. The corresponding displacements can be formulated directly in closed form as a function of the depth of the site.

For the TAMU footing, cone model impedance functions were calculated using the MATLAB scripts provided by Wolf and Deeks (2004). To develop a cone model, a profile view of the soil/foundation system was subdivided into horizontal layers, and each layer is described by seven parameters: layer type, layer thickness, radius of foundation, shear modulus of soil, Poisson's ratio of soil, mass density of soil, and material damping ratio of soil. Layering decisions for the profile were typically determined by two considerations: 1) approximating the soil material profile by a stack of layers each with homogenous material properties, and 2) satisfying the criterion of Wolf and Deeks (2004) that the layers of soil adjacent to an embedded foundation be no thicker than 1/10 of the smallest wavelength generated by the vibrating footing.

Since the cone model impedances are calculated for circular disk (axisymmetric) foundations, the TAMU square footing was converted to an equivalent disk for cone computations. The equivalency was based upon contact area for translational modes (vertical, horizontal), and moment of inertia for the rocking mode.

Briaud and Gibbens (1994) provide mass density information for the sand layers at the site, while the mass density for the hard clay was assumed to be 1,886 kg/m^3. For Poisson's ratio, a value of 0.33 was assumed for the sand layers, and a value of 0.45 for the hard clay below the water table. Material damping was assumed to be 3% for all layers based on soil descriptions from Briaud and Gibbens (1994) and typical values provided by Prakash and Puri (1988). The shear modulus of each layer was calculated from the mass density and shear wave velocity. The mass density was discussed above. The free-field shear wave velocities were measured by Tran and Hiltunen (2011) at the TAMU site via surface wave tests.

Using the cone model impedances, the vertical displacement of the footing was computed as described above using Equation 1 and the results are presented in Figures 11 and 12. In general, there is good agreement between the measured and predicted displacement results and the agreement is particularly good for frequencies below about 50 Hz.

Again, using the cone model impedances, the coupled horizontal sliding displacement and rocking rotation of the foundation were computed as described above using Equation 2 and the results are presented in Figures 13-16. In general, there is good agreement between the measured and predicted response results. The agreement is particularly good for frequencies up to 20 Hz, with deviations occurring at higher frequencies. Over the range of frequencies available, the measured responses appear nearly linear with variation in frequency, while there is a slight curvature in the predicted responses.

4.2 *PILAY Models*

PILAY computes the dynamic stiffness and damping coefficients (impedance functions), internal forces, and displacements for all vibration modes for a vertical pile embedded in layered soil and based on the theory published by Novak and Aboul-Ella (1978). The model derives the soil reactions from a continuum and represents the pile by finite elements. The model is approximate but incorporates the important variation of soil properties with depth. The soil is composed of horizontal layers that are homogeneous, isotropic, and linearly viscoelastic with properties that are constant within each layer but may be different in individual layers. The pile is vertical, linear elastic, and of circular cross section that is bonded to the soil.

Input properties of the pile include length, Young's modulus, Poisson's ratio, and unit weight. The thickness, shear wave velocity, Poisson's ratio, unit weight, and material damping coefficient are required for the soil layers around the pile and below the tip. The program can analyze three model options: 1) a pile in a layered media, 2) a pile within a parabolic distribution of soil shear modulus, and 3) a rigid body surrounded by and underlain by a layered media. The TAMU footing was analyzed with this last option using the soil layering determined in the site characterization and using properties discussed in the previous section on cone models.

Like the analysis discussed above for cone models, the PILAY impedance functions were used as input to Equations 1 and 2 to compute the foundation responses and the results are presented in Figures 11-16. As with the cone models, the PILAY model predictions of both vertical and horizontal displacement are in good agreement with the measured footing displacements. The deviations in the horizontal displacements at higher frequencies are like those of the cone. However, the PILAY model produces considerable underestimation of the rocking response of the footing (Figures 15 and 16). A more detailed examination of the calculations reveals that the PILAY rocking impedance functions are substantially larger than those produced by the cone, Apsel and Luco, and Gazetas models, thus the lower computed rotation.

4.3 *Apsel and Luco Models*

Apsel and Luco (1987) present an integral equation approach to solve for the dynamic response of embedded foundations of arbitrary shape. The soil is modeled as viscoelastic and consists of parallel layers overlying a half space. The foundation is assumed to be rigid and perfectly bonded to the soil. To validate and illustrate use of the technique, the paper tabulates in dimensionless form the impedance functions for cylindrical foundations of radius a embedded to a depth h in a uniform viscoelastic half space for embedment ratios of h/a of 0, 0.25, 0.5, 1 and 2. Full contact between the foundation and soil was assumed. The impedance functions are referred to the center of the bottom of the foundation and normalized by the radius a and the shear modulus of the half space soil.

Since the Apsel and Luco (1987) tabulated impedance functions require a uniform half space as input, as opposed to the full site characterization information used in the cone and PILAY models, a different approach was used to present the results in Figures 11-16. To begin, impedance functions and predicted foundation motions were solved in a MATLAB code for a range of half space shear wave velocities and using Poisson's ratio=0.33, and mass density=1558 kg/m^3. A value of shear wave velocity=120 m/s was found to provide a good overall fit between the predicted and measured motions and these results are presented in Figures 11-16. A more detailed discussion of the effect of half space modulus is found in a section below.

4.4 *Gazetas Models*

Gazetas (1991) presents a series of algebraic formulas, tables, and dimensionless charts for computing the impedance functions of foundations under dynamic loading. The methodology is based on the results of both rigorous and approximate formulations. Solutions for all translational and rotational modes of vibration are provided for six soil/foundation systems: 1) a foundation of any solid shape resting on the surface of a homogeneous half space, 2) a foundation with any solid base shape and partially or fully embedded in a homogeneous half space, 3) circular and strip foundations on the surface of a homogeneous soil stratum underlain by bedrock, 4) circular and strip foundations partially or fully embedded in a homogeneous stratum underlain by bedrock, 5) square and strip foundations on the surface of inhomogeneous profiles in which the modulus increases smoothly with depth, and 6) laterally loaded single floating piles in two inhomogeneous and a homogeneous stratum or half space.

Like Apsel and Luco (1987), the Gazetas (1991) impedance functions require a uniform half space as input, as opposed to the full site characterization information used in the cone and PILAY models. Gazetas (1991) also requires an assessment of the effective embedment of the foundation. Again, impedance functions and predicted foundation motions were solved in a MATLAB code for a range of half space shear wave velocities and embedment depths and using Poisson's ratio= 0.33 and mass density=1558 kg/m^3. Full embedment and a value of shear wave velocity=135 m/s were found to provide a good overall fit between the predicted and measured motions and these results are presented in Figures 11-16. A more detailed discussion of the effects of half space modulus and embedment are found in the following sections.

4.5 *Effect of Half Space Modulus*

As discussed above, the impedance function models of Apsel and Luco (1987) and Gazetas (1991) require a uniform half space as input and do not incorporate the variation of soil properties with depth. The results from these models presented in Figure 11-16 were found to best predict the measured footing responses. A more detailed look at the effect of half space modulus on foundation response was conducted by comparing the magnitude of the predicted vertical, horizontal, and rotation responses with the measurements using the Gazetas (1991) impedance functions and a range of shear wave velocities from 120 to 150 m/s. As expected, the shear wave velocity had a significant effect on the motions, and it appeared reasonable to assume a value of 135 m/s provides a good overall agreement with the measurements. As reported by Tran and Hiltunen (2011), there is significant variation of shear wave velocity in this soil profile and a shear wave velocity of 135 m/s is representative of soil in the uppermost 2 m. While the agreement between predicted and measured results are not as good as for the cone models, it is interesting to note that it is possible to approximate the response via a uniform half space. However, while it may be possible to find an empirical approach, it is not obvious how one would determine this representative velocity value a priori in a design situation and without the benefit of field response measurements.

4.6 *Effect of Embedment*

As discussed above, the Gazetas (1991) impedance function models require an assessment of the effective embedment of the foundation. The results from these models presented in Figures 11-16 assuming full embedment were found to best predict the measured footing responses. A more detailed look at the effect of embedment on foundation response was conducted by comparing the magnitude of the predicted vertical, horizontal, and rotation responses were compared with the measurements using a range of conditions from a footing on the ground surface, a footing in a trench (minimal sidewall contact), and three levels of sidewall contact up to full embedment. The results indicated that the effect of embedment is significant, if not dramatic. It was obvious that a model assuming a footing on the ground surface is not appropriate for this embedded foundation. It was also interesting to note that the predicted vertical response was the same for all levels of embedment from trench to full. Finally, it appeared reasonable to conclude that a model that assumes full embedment and sidewall contact produced the best overall agreement with the measurements.

5 CONCLUSIONS

A square and embedded shallow foundation was dynamically loaded at the National Geotechnical Experiment Site (NGES) on the campus of Texas A&M University (TAMU) via the T-Rex and ANCO dynamic loading devices and the measured results were compared with results computed from cone models of the soil/foundation system. Based upon the experimental and analysis results, the following conclusions are appropriate:

- The measured responses of the footing under dynamic load indicate that a rigid body motion model for movement of the footing is appropriate.
- A rigid body model based upon a single-degree-of-freedom (SDOF), mass-spring-dashpot concept, employing a dynamic impedance function computed using free-field shear wave velocity values measured at the site with surface wave tests, provides a good assessment of the dynamic response of the foundation under vertical excitation.
- A rigid body model based upon a two-degree-of-freedom (2DOF), mass-spring-dashpot concept, employing dynamic impedance functions computed using free-field shear wave velocity values measured at the site with surface wave tests, provided a good assessment of the dynamic response of the foundation under horizontal excitation.
- Overall, the cone models produced the best predictions of the measured field responses and the predictions can be made a priori using the layered soil profile from in situ measurements.
- All four methodologies produced good predictions of the vertical and horizontal motions of the foundation.
- For horizontal excitation, the agreement between measured and predicted responses is particularly good for frequencies up to 20 Hz, with deviations occurring at higher frequencies. Over the range of frequencies available, the measured responses appear nearly linear with variation in frequency, while there is a slight curvature in the predicted responses.
- The rocking motions were also well predicted using cone and half-space models, while the PILAY predictions of rocking were quite different from the measurements due to apparent differences in the computed impedance functions.
- The Gazetas model results suggested that full embedment and full contact of the foundation and soil produced the best representation of the field behavior. It was possible to find one representative half-space modulus for the models to approximately match the field measurements for all modes of vibration, but it was not obvious how one would determine this modulus value a priori in a design situation and without the benefit of field response measurements.

6 REFERENCES

Apsel, R.J. and Luco, J.E. (1987), "Impedance Functions for Foundations Embedded in a Layered Medium: An Integral Equation Approach," *Earthquake Engineering and Structural Dynamics*, Vol. 15, pp. 213-231.

Briaud, J. and Gibbons, R.M., (1994), "Data and Predictions Request for the Spread Footing Prediction Event," *Predicted and Measured Behavior of Five Spread Footings On Sand: Proceedings of a Prediction Symposium, Geotechnical Special Publication No. 41,* ASCE, June, pp. 11-85.

Gazetas, G. (1991), "Foundation Vibrations," Chapter 15 in *Foundation Engineering Handbook*, 2nd ed., Edited by H.-Y. Fang, Van Nostrand Reinhold, New York, pp. 553-593.

Novak, M. and Aboul-Ella, F. (1978), "Impedance Functions of Piles in Layered Media," *Journal of the Engineering Mechanics Division,* ASCE, Vol. 104, No. EM6, June, pp. 643-661.

Prakash, S. and Puri, V. K. (1988), *Foundations for Machines: Analysis and Design*, John Wiley & Sons, Inc., New York, 656 pp.

Tileylioglu, S., Stewart, J.P., and Nigbor, R.L. (2011), "Dynamic Stiffness and Damping of a Shallow Foundation from Forced Vibration of a Field Test Structure," *Journal of Geotechnical and Geoenvironmental Engineering*, American Society of Civil Engineers, Vol. 137, No. 4, April, pp. 344-353.

Tran, K.T. and Hiltunen, D.R. (2011), "An Assessment of Surface Wave Techniques at the Texas A&M National Geotechnical Experimentation Site," *Risk Assessment and Management in Geoengineering, Geotechnical Special Publication No.224*, C. H. Juang, K. K. Phoon, A. J. Puppala, R. A. Green, and G. A. Fenton, Eds., American Society of Civil Engineers, pp. 859-866.

Wolf, J.P. and Deeks, A.J. (2004), *Foundation Vibration Analysis: A Strength-of-Materials Approach*, Elsevier, 218 pp.